Electrochemical Synthesis of Titanium Dioxide Nanoparticles for UV Radiation Protection

Jaewoo Lee[a], Sangyoon Lee[a], Sung Oh Cho[a*]

[a]Dept. of Nuclear and Quantum Engineering, Korea Advanced Institute of Science and Technology (KAIST),
291, Daehak-ro, Yuseong-gu Daejeon, Republic of Korea, 34141
[*]Corresponding author: socho@kaist.ac.kr

1. Introduction

Exposure from UV radiation can cause serious damage to human skin. The UV spectrum consists of three ranges depending on its wavelength; UVA (315-400 nm), UVB (280-315 nm), and UVC (100-280 nm). The UVC rays are mostly shielded by the ozone layer, while the UVA and UVB rays reach the ground surface. Therefore, it is important that UV radiation has to be shielded for protection, particularly UVA and UVB.

Meanwhile, titanium dioxide nanoparticles (TiO_2 NPs) are of great interest in cosmetics, solar cells, and coatings with relation to their photocatalytic activity, chemical stability, and non-toxicity. In particular, their extraordinary ability to block UV radiation was reported [1]. The application of TiO_2 NPs varies depending on their crystal structures. TiO_2 NPs commonly have three polymorphs; anatase, rutile, and brookite. Of the above three crystal forms, the rutile TiO_2 NPs are used in sunscreens with their UV absorption and scattering effect [2].

Although there are many methods to synthesize TiO_2 NPs, simple, green, and economical processes for the preparation of TiO_2 NPs are still under development. Conventionally, thermal decomposition, hydrothermal synthesis, sol-gel synthesis, and co-precipitation methods can prepare various metal oxide nanoparticles (MONPs). However, these methods are related to several limitations, for instance, the use of high-temperature and costly facilities, long-lasting and tricky multi-process, use of highly consumptive materials, induction of environmental issues.

Here, we propose a one-step electrochemical method (i.e., anodization) to synthesize mass productive TiO_2 NPs with the rutile phase for UV radiation protection. Furthermore, we reveal the ability of fabricated TiO_2 NPs to absorb the UV radiation. The anodization process is deployed at low temperatures and is a simple, fast, economical, and eco-friendly process. We believe such technology has great potential to be applied in MONPs industries.

2. Experimental Section

2.1 Materials

Titanium wire (0.8 mm in diameter and 99.9% purity) was procured from Nilaco Corporation, Japan. Reagent-grade potassium chloride (KCl) and hydrochloric acid (HCl) were purchased from Sigma-Aldrich, USA and Daejeong, Korea, respectively. The electrolyte was prepared with deionized (DI) water.

2.2 Sample Preparation

Anodization of titanium wire was conducted in 1 M KCl aqueous solution with or without a small amount of HCl additive. Prior to anodization, titanium wire was cleaned by sonicating in acetone and ethanol each for 5 min followed by rinsing with DI water and drying with an air stream. Anodization was performed in a two-electrode system with a stainless steel beaker (Ø 50 mm × 55 mm) as a cathode and titanium wire as an anode at room temperature as depicted in Fig. 1. Anodization voltage was kept constant using a DC power supply. During anodization, the titanium wire was converted into precipitate and this precipitate was firstly centrifuged with 10,000 rpm for 20 min after anodization. The centrifuged precipitate was washed (and dispersed) with DI water and sonicated in DI water for 5 min to remove any type of impurities. This process was repeated 3 times. Then, the obtained gel-type matter was kept in an oven at 60°C overnight and collected in the form of soft powder.
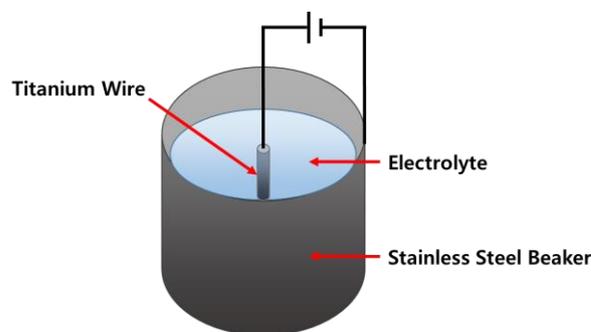
Fig. 1. Schematic view of anodization system.

2.3 Sample Characterization

The produced powder was characterized using field emission scanning electron microscope (FESEM, Magellan400, FEI, USA) and X-ray diffractometer (XRD, SmartLab, RIGAKU, Japan) analysis. Energy-dispersive X-ray (EDX) spectrum was obtained with FESEM. The particle size of powder was directly measured from the FESEM images with the diameters of at least 100 particles. XRD analyzed the crystal structure of particles with Cu Kα radiation (1.5406 Å wavelength) at 40 kV. The UV protection property of

the powder was evaluated using an ultraviolet-visible spectrophotometer (UV-Vis, Lambda 1050, Perkin Elmer, USA). UV-Vis analysis was conducted by measuring the absorbance of UV rays according to wavelength.

3. Results and Discussion

3.1 Fabrication of Titanium Dioxide Nanoparticles

Some white precipitate occurred when a titanium wire was anodized in 1 M KCl aqueous electrolyte at 15 V for 3 min with a stainless steel beaker as the cathode. After anodization, the edge of titanium wire became very sharp like a needle. With several times of employing centrifugation and sonication white powder was obtained (Fig. 2a). FESEM image presents particle size distribution, whose average diameter is ~26.6 nm (Fig. 2b). In addition, the EDX spectrum confirms that the main element components of powder are Ti and O whose atomic compositions are ~34.1% and ~65.9%, respectively. This supports the formation of TiO_2 NPs (Fig. 2c). The K and Cl peaks are due to the electrolyte and the C peak is due to carbon tape. Consquently, we verified the powder comprises TiO_2 NPs.

Further investigation for identifying the crystal structure of the TiO_2 NPs was performed using XRD analysis. Fig. 3 shows that the XRD pattern of titanium oxide nanoparticles has no clear peaks over the entire 2-theta range. Therefore, the TiO_2 NPs produced in 1 M KCl solution at 15 V are amorphous. However, amorphous TiO_2 NPs are rarely used in UV radiation protection so fabricating the crystalline titanium oxide nanoparticles, particularly rutile, is an indispensable task in terms of UV protection.
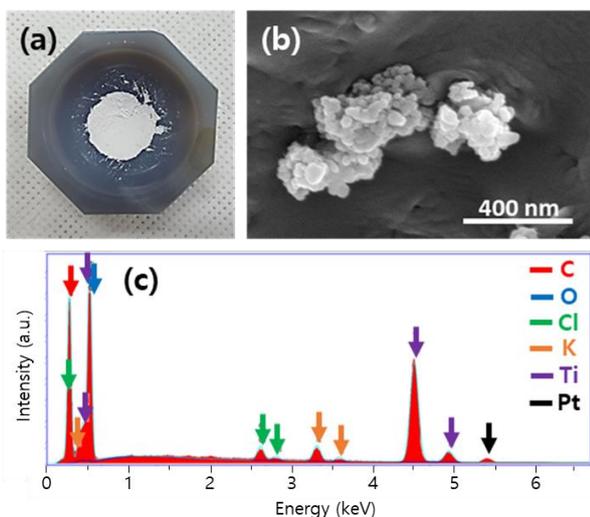
Fig. 2. (a) Digital photograph, (b) FESEM image, and (c) EDX spectrum of TiO_2 NPs obtained via anodization in 1 M KCl aqueous electrolyte at 15 V for 3min.
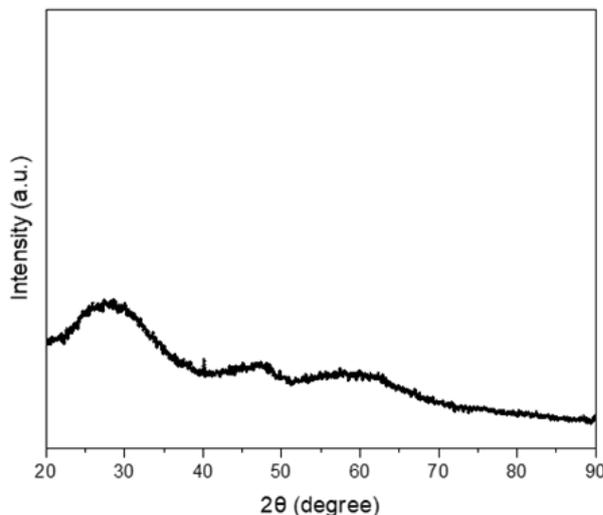
Fig. 3. XRD pattern of TiO_2 NPs obtained via anodization in 1 M KCl aqueous electrolyte at 15 V for 3 min.

3.2 Effects of Anodization Parameters on Crystallinity

The properties of oxide can be changed by controlling the anodization parameters. Such parameters can be temperature, time, electrolyte composition, or voltage. First of all the duration effect on the crystallinity of nanoparticles was investigated by changing anodization time 5, 10, and 15 min. When the titanium wire is anodized for 5 min, the spectrum is widely broadened and there are no clear peaks (Fig. 4a). However, when the anodization time increase, some peaks are present and match with anatase (ICDD PDF No. 00-064-0863) (Fig. 4b,c). This suggests amorphous TiO_2 NPs grow in crystalline structure as anodization time increases. Furthermore, when anodization is in process, the temperature of electrolyte reaches up to ~90°C due to local exothermic heat [3]. The local heat may help nucleation and crystallization of amorphous TiO_2. It means amorphous TiO_2 is transformed to anatase as anodization is more in progress.

Another one is the effect of the chemical composition of electrolytes due to acid additive. Fig. 5 shows the XRD spectra of each case with different amounts of HCl additive in the electrolyte. When anodizing a titanium wire for 15 min without any HCl addition, broad peaks show that anatase is produced with very low crystallinity (Fig. 5a). On the other hand, if there is a small amount of HCl in the electrolyte, the crystallinity becomes much better (Fig. 5b-d). In addition, in the cases of HCl addition, the rutile (ICDD PDF No. 01-077-0443) phase appears as well as anatase. However, if a large amount (more than 1 M) of HCl is added to the electrolyte, no nanoparticles are produced. This may be due to the lack of oxygen species because the HCl reacts with them. Respect to the effect of HCl additive, one plausible explanation is that neutralization and solubility affect crystallization. As HCl reacts with OH^-, the heat of neutralization is generated and becomes the energy
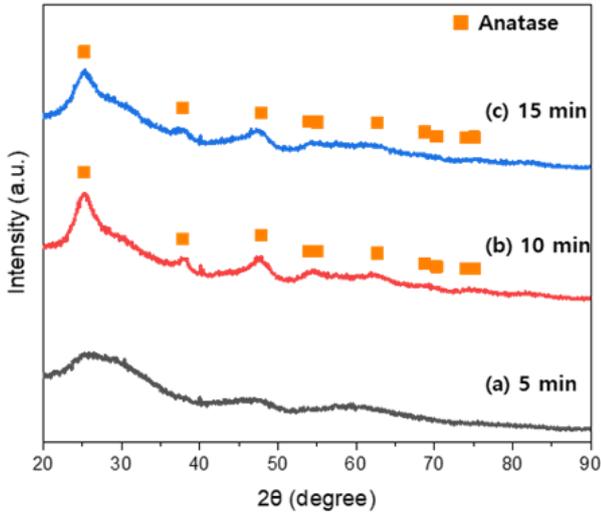
Fig. 4. XRD patterns of TiO$_2$ NPs obtained via anodization in 1 M KCl aqueous electrolyte at 15 V for each duration.
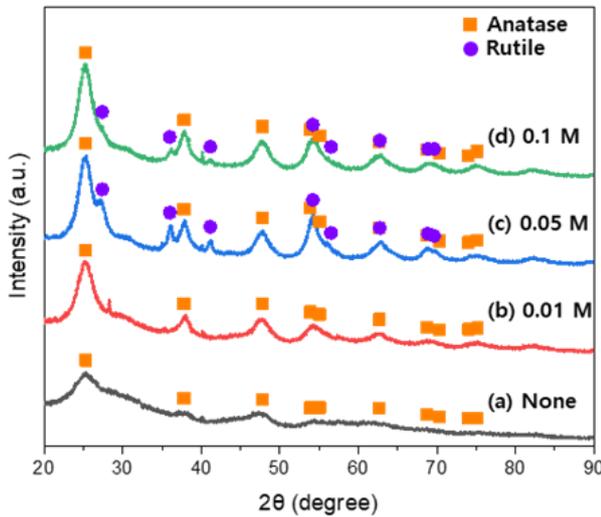
Fig. 5. XRD patterns of TiO$_2$ NPs obtained via anodization in 1 M KCl aqueous electrolyte containing each concentration of HCl additive at 15 V for 15 min.
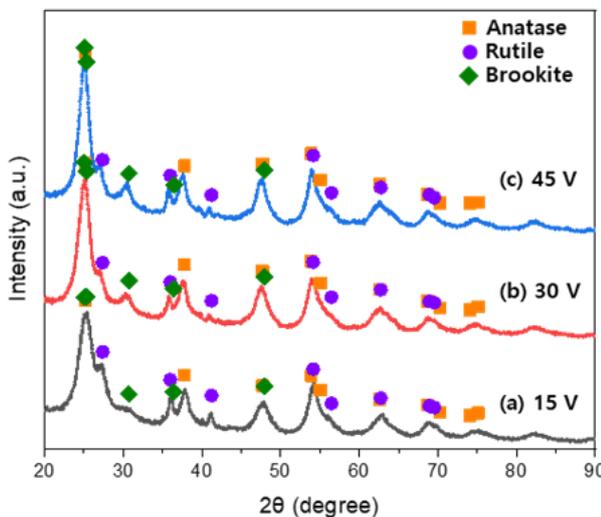
Fig. 6. XRD patterns of TiO$_2$ NPs obtained via anodization in 1 M KCl aqueous electrolyte at each voltage for 15 min.

source of crystallization. Likewise, the HCl addition lowers the solubility of electrolyte to the precipitate. This leads faster reaching supersaturation. Subsequently, nucleation is achieved and crystal growth is carried out [4]. It is found the peaks match the best in the case of 0.05 M HCl addition.

The last effect is that of applied voltage during anodization. The voltages were applied at 15, 30, and 45 V respectively. The time lasted 15 min and HCl was added 0.05 M. Obtained XRD results are given in Fig. 6. At low voltage (15 V) anatase and rutile are found but another crystal structure is identified at higher voltages. A clear peak of around 30° is well matched on brookite (ICDD PDF No. 01-076-1937). Brookite may be caused by phase transformation, with relatively stable anatase and rutile receiving energy from high voltage. Furthermore, it is worth noting the nanoparticles are slightly more crystalline at higher voltages.

3.3 Mechanism of Nanoparticles Formation

We have found TiO$_2$ NPs are synthesized when anodizing a titanium wire in KCl aqueous electrolyte. The anodization process generally is explained with the competition of oxidation and etching reaction. A possible process of TiO$_2$ NPs formation is expressed as follows:

$$Ti^{4+} + 4OH^- \rightarrow TiO_2 + 2H_2O \qquad (1)$$
$$Ti^{4+} + 2O^{2-} \rightarrow TiO_2 \qquad (2)$$
$$TiO_2 + 6Cl^- + 4H^+ \rightarrow [TiCl_6]^{2-} + 2H_2O \qquad (3)$$
$$Ti^{4+} + 6Cl^- \rightarrow [TiCl_6]^{2-} \qquad (4)$$

Eq. (1) and (2) are general forms of oxidation in the metal-water system and Eq. (3) and (4) are etching reactions, which are chemical etching and field-assisted etching respectively. The balance of four reactions makes titanium oxide nanoparticles in KCl aqueous electrolyte. A schematic view of the mechanism of TiO$_2$ NPs formation is illustrated in Fig. 7. For simplicity, the cathodic part is depicted as an electrode structure similar to the anode.

(I) The titanium wire is used as anode and is in contact with the counter electrode through electrolyte containing chloride ions (Cl$^-$).

(II) As soon as voltage is applied between two electrodes, titanium ions, mostly Ti^{4+}, are created and water is electrolyzed to produce H$^+$ and OH$^-$. Moreover, there are O^{2-} in the process and hydrogen gas evolves at the cathode.

(III) A thin titanium oxide layer is developed on the titanium wire surface due to a combination of Ti^{4+} and anions (OH$^-$ and O^{2-}) (i.e., oxidation). The titanium oxide layer is dropped in nanoscale by etching reaction.

(IV) The titanium oxide is ultimately extracted as TiO$_2$ NPs.
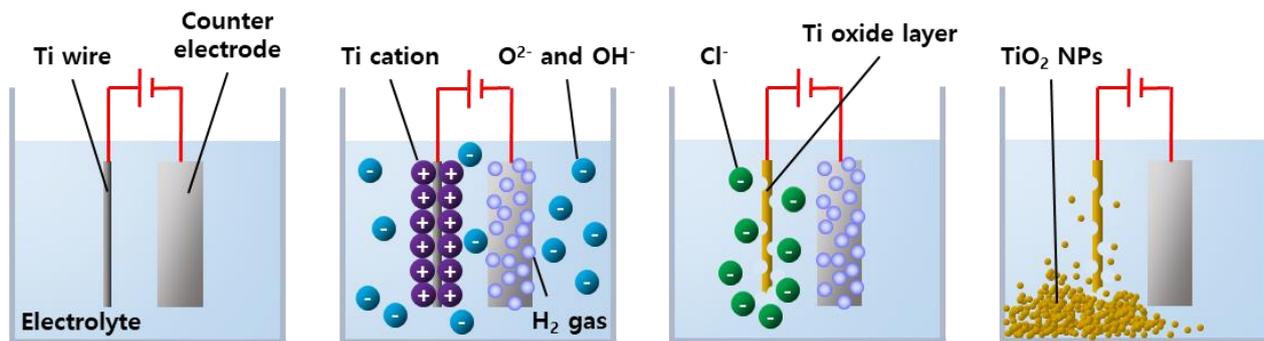
Fig. 7. Schematic diagram depicting the formation mechanism of titanium oxide NPs via anodization.

3.4 UV Absorption Analysis

In order to evaluate the property for UV radiation protection, the absorbance of waves with wavelength was measured in the UV-visible light region. The absorbance is calculated as expressed in Eq. (5).

$$\text{Absorbance} = \log\frac{I_0}{I}$$

where, I_0 is the initial intensity of wave before being absorbed into the substance and I is the final intensity of wave after being absorbed. Fig. 8 shows the wave absorbance of TiO_2 NPs synthesized by anodization according to wavelength. All TiO_2 NPs including the rutile phase absorbed significantly the UV rays in the range of 200-350 nm. This region corresponds with the UVB region and is quite appropriate for the UVA and UVC regions. In particular, the absorbance is approximately unity in the UVB region (~300 nm), so it suggests 90% of the UV is absorbed. In addition, the most crystalline TiO_2 NPs case (i.e., 45 V for applied voltage) exhibits slightly higher UVB absorbance. As a result of the UV absorption evaluation, our TiO_2 NPs prepared by anodization are verified to be high potential materials for UV radiation protection.
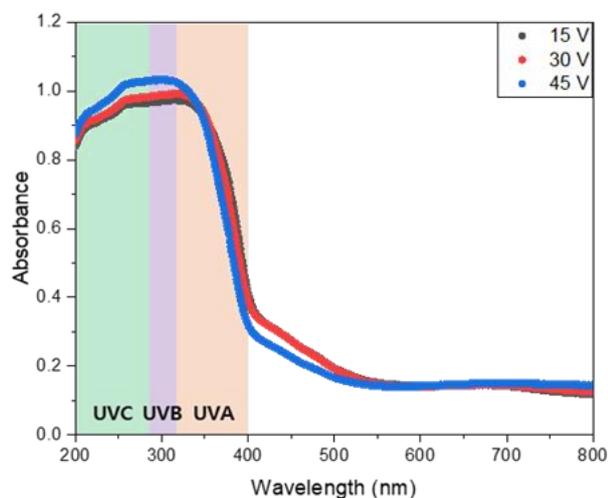
Fig. 8. UV-Vis absorption of TiO_2 NPs obtained via anodization in 1 M KCl aqueous electrolyte containing 0.05 M HCl additive at constant voltage for 15 min.

4. Conclusions

This study has presented a promising method to prepare TiO_2 NPs using simple anodization. Amorphous TiO_2 NPs are produced when a titanium wire is anodized at room temperature in 1 M KCl aqueous solution for 5 min with constant voltage 15 V. As anodization time increases, the nanoparticles become crystallized and anatase phase occurs. Also, a small amount of HCl additive in electrolyte makes it possible to produce more crystalline TiO_2 NPs. It initiates the rutile phase of NPs due to the heat of neutralization. Furthermore, higher applied voltage transforms anatase or rutile to brookite and achieves a significantly crystalline structure.

The formation mechanism of TiO_2 NPs via anodization in chloride-based electrolytes is explained by oxidation and etching reactions. However, it is necessary not only to establish a clear theory for NPs formation but also to synthesize pure rutile TiO_2 NPs.

Meanwhile, our TiO_2 NPs fabricated by anodization have outstanding UVB absorbance, which is about 90% of absorption. It is noteworthy TiO_2 NPs produced by the economical, one-step, and eco-friendly anodization method have significant potential to be used in UV radiation protection.

REFERENCES

[1] R. Kessler, Engineered Nanoparticles in Consumer Products: Understanding a New Ingredient, Environmental Health Perspectives, Vol.119(3): e120, 2011.
[2] C. F. Bohren and D. R. Huffman, Absorption and Scattering of Light by Small Particles, Wiley-VCH Verlab GmbH & Co. KGaA, 1983.
[3] G. Ali, Y. J. Park, J. W. Kim, and S. O. Cho, A Green, General, and Ultrafast Route for the Synthesis of Diverse Metal Oxide Nanoparticles with Controllable Sizes and Enhanced Catalytic Activity, ACS Appl. Nano Mater., Vol.1, pp.6112-6122, 2018.
[4] J. S. España, Crystallization in Acid Media: from Nanoparticles to Macrocrystals, Instituto Geológico y Minero de España, Vol.1: e28760, 2017.